



Comparison of Air Pollutants Between Kolkata and Siliguri, India, and Its Relationship to Temperature Change

Kuntal Biswas¹ · Arpita Chatterjee² · Jyotibrata Chakraborty³ 

Accepted: 15 October 2020

© Springer Nature Switzerland AG 2020

Abstract

The rapid pace of economic growth and urbanization in Kolkata affects both the people and places. As the city grows physically, it counters several environmental degradations including air pollution. Siliguri, the gateway to north-eastern India, is also under deplorable environmental conditions with a growing industrial sector and rapid urbanization. This study aims to portray the current air pollution situation with seasonal variation in three zones (two from Kolkata and one from Siliguri) as it evaluates the present level of different air pollutants like particulate matter (PM), carbon monoxide, nitrogen dioxide, and sulfur dioxide. The result of the seasonal analysis shows the critical level of air pollutants, especially PM_{2.5} and PM₁₀, has reached its highest concentration during the post-monsoon season in the Rabindra Bharati University zone (363.5 and 295.4 µg/m³ respectively during the daytime) of Kolkata, and thereafter, monthly characteristics of the most variant seasonal pollutants were examined in the studied areas. These seasonal fluctuations of pollutants reflect the impact of meteorological conditions, as such pollutants coming out from different sources are also raising temperatures. Therefore, this work also tries to justify the environmental pollution scenario using Spearman's rank correlation coefficient method between the average temperature of a day (°C) and the level of air pollutants (µg/m³) like PM_{2.5} and CO, separately. Positive values of correlations may indicate the contemporary status of the air quality, as well as the environmental state, that will be an important basis for further regional studies on air quality and distribution of sources.

Keywords Air pollution · Seasonal variation · Particulate matter · Spearman's rank correlation

Introduction

Kolkata, the city of joy, situated on the banks of the Hooghly river, in the Gangetic belt, is one of the fastest growing

Electronic supplementary material The online version of this article (<https://doi.org/10.1007/s41651-020-00065-4>) contains supplementary material, which is available to authorized users.

✉ Jyotibrata Chakraborty
jyotibratachakraborty7@gmail.com

Kuntal Biswas
kbis_75@yahoo.co.in

Arpita Chatterjee
arpitachatterjee2008@gmail.com

¹ Department of Physics, Dum Dum Motijheel College, Kolkata 700074, India

² Department of Geography, Dum Dum Motijheel College, Kolkata 700074, India

³ Geoinformatics and Remote Sensing Cell, West Bengal State Council of Science and Technology, Government of West Bengal, Kolkata, India

metropolises in India and has been suffering from air pollution (Spiroska et al. 2011). An analysis from different sources of air pollution in Kolkata has revealed that motor vehicles are the leading contributor to the pollution (51.4%) followed by industry (24.5%) and dust particles (21.1%), respectively (Chakraborty 2014). Siliguri, the gateway to north-east India, is at a distance nearly 559 km from Kolkata also experiencing severe air pollution at present. Siliguri is the second largest Himalayan foothills zone city in West Bengal, very well known for commercial activities. A recorded Air Quality Index (AQI) value of 343.6 in February 2018 by the Central Pollution Control Board—India is a strong indication of poor air quality. As the cities grow physically to keep up with its economic growth, it counters several environmental degradations. Air pollution is one of them. A report published by the World Health Organization in 2002 shows around 4.6 million people die each year because of the direct impact of air pollution (WHO 2002). Rapid and unplanned urbanization is making this problem more acute in many megacities in developing countries (UNEP 1999).

One of the main factors leading to the increase in air pollution is transportation (Mondal et al. 2000). An abundance of

poorly maintained vehicles, use of petrol fuel, and poor controls is making transportation the major air-polluting sector (Mukherjee and Mukherjee 1998; Kazimuddin and Banerjee 2000). Development of many branches of industry also resulted in huge atmospheric emissions of such pollutants such as particulate matter (PM) including PM_{2.5} (particles with aerodynamic diameter $\leq 2.5 \mu\text{m}$) and PM₁₀ (particles with aerodynamic diameter $\leq 10 \mu\text{m}$) and gas pollutants—sulfur dioxide (SO₂), nitrogen dioxide (NO₂), and carbon monoxide (CO). These pollutants remain of concern because of their effect on the environment, climate, and human health (Xie et al. 2016). Being principal pollutants, they may have a direct impact on air quality (Filonchik and Yan 2018; Guan et al. 2019). But, it is high PM_{2.5} values that are of main concern because it has a dramatic effect on human health, leading to lung cancer, cardiopulmonary, cardiovascular, and respiratory diseases—all of which result in premature mortality (Ren et al. 2010; De et al. 2013; D'amato et al. 2016).

Many studies have examined air pollution levels in Kolkata and Siliguri from different viewpoints. Some of the studies start with general aspects of the geography and climate that influences the pollution levels immensely followed by those with startling effects of air pollution. The air pollution situation in Kolkata and Siliguri has been analyzed from different perspectives, but the present study aims to compare the contemporary air pollution situation in these two megacities by analyzing the present level of different air pollutants such as particulate matter (PM), carbon monoxide (CO), nitrogen dioxide (NO₂), and sulfur dioxide (SO₂). Based on recorded pollutant data by the West Bengal Pollution Control Board, continuous monitoring of air quality has been carried out to assess the variation of air pollutants (PM_{2.5}, PM₁₀, CO, NO₂, and SO₂) with seasonal change at selected geographical locations.

The data of each air pollutant from 3 stations (2 from Kolkata and 1 from Siliguri) were taken into consideration for two times in a day (11 AM and 11 PM) to know their day and night variations for each zone for three different seasons. This study also attempts to establish a relationship between air pollution (in $\mu\text{g}/\text{m}^3$) and metrological factors such as the average temperature by using the Spearman's rank correlation. In this particular work, Remote Sensing and Geographical Information System (GIS) emerged as a very essential tool and proved to be quite convenient in mapping land use/land cover (LULC) forms and their changes with time. Such techniques are cost-effective in dealing with a phenomenon like spatial and temporal variability of LULC in and around Kolkata and Siliguri municipal corporation areas in order to understand the nature of urbanization, the effect of vehicular movement, increasing land surface temperature, and its influence on existing air pollution. This will enable us to assess the changes not only in air quality but also in the surrounding environment, identify the potential sources of solid

particles in atmospheric air, and also help to develop the preventive and control measures to improve air quality in the selected regions.

Materials and Methods

Study Area

The study areas are chosen based on the availability of recorded pollutant data and for a better representation of the pollution scenario. Therefore, two study areas have been selected from Kolkata; these are Rabindra Bharati University (RBU) zone located in the north of Kolkata Municipal Corporation (KMC) and Victoria Memorial (VICT) zone in the middle of KMC. Another study area is chosen at Babupara (SILG) zone in Siliguri Municipal Corporation (SMC). Presently, Kolkata and Siliguri municipal corporations and their surrounding areas are witnessing a rapid and substantial amount of change in their LULC configuration. Rapid urbanization at the cost of destroying greenery has been accelerating air pollution in these areas (Fig. 1).

Land Use/Land Cover Classification and Retrieval of Land Surface Temperature

Two problems are concerned with modern land use dynamics. Firstly, the intensive use of land to achieve the maximum possible profit. Secondly, changes in land use from rural to urban, which involves the actual loss of land from a particular land use that should be permissible only after estimating its production and exploring the possibilities of its compensation (Siddhartha and Mukherjee 2004). In this regard, analysis of temporal built-up growth and its spatial components using multi-spectral satellite imagery is particularly helpful because it provides efficient support for wide landscape analysis with regularly updated and easily accessible data. Thus, in this study at first, the territorial boundary of KMC and SMC (ward maps) were procured from respective official websites of each municipal corporation and digitized accordingly. Later pre-processed Resourcesat 2 Linear Imaging Self Scanning III sensor images (spatial resolution 23.5 m, path 107 and 108; row 053 and 056) of 2006 and 2016 were obtained from National Remote Sensing Centre-Bhuvan earth observation data (n.d.) archive covering Kolkata and Darjeeling-Jalpaiguri region and subsequently processed to produce Standard False Colour Composite (SFCC) images in ESRI ArcGIS platform. Based on the SFCC images, the LULC feature classes of selected years have been generated by on-screen digitization within the areas of interest for a

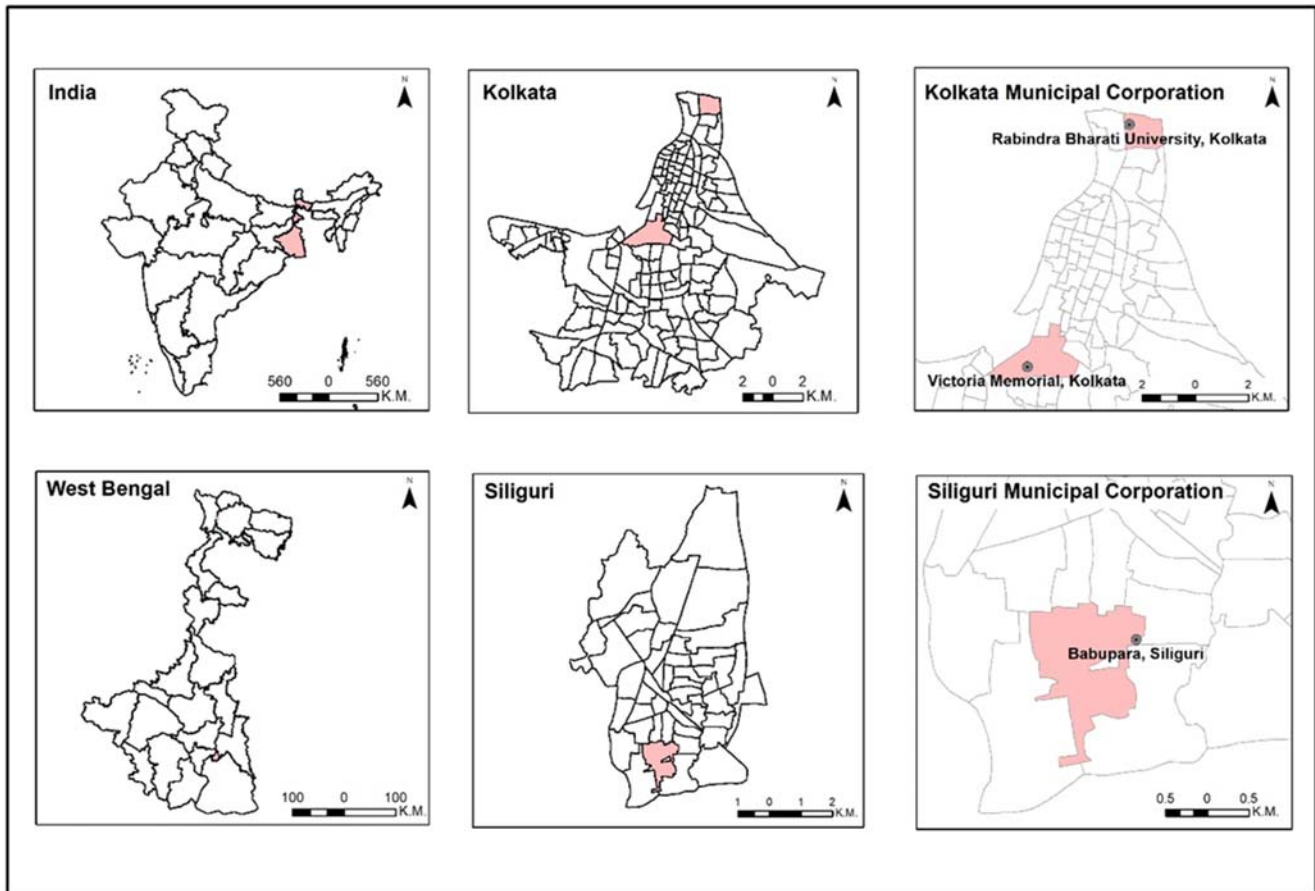


Fig. 1 Location map showing study areas

transparent understanding of the dynamic phenomenon such as LULC change, built-up growth, and distribution of land surface temperatures.

Land surface temperature (LST) can supply primary information on the surface substantial property and environment. For instance, the thermal infrared data are efficiently used to follow in the temperature differences between urban and rural areas in India (Weng et al. 2004) and to delineate urban heat pockets which are also developed in consonance with intensified LULC conversion in and around the built-up areas. Therefore, LST analysis was carried out in the studied areas to figure out places with high surface temperature using LANDSAT 8 Operational Land Imager and Thermal Infrared Sensor (TIRS) sensor data (spatial resolution 30 m and 100 m, path 138 and 139; row 041 and 044) of 2018 which were derived from the United States Geological Survey Earth Explorer repository (n.d.), with a single scene containing the entire studied stretch. National Aeronautics and Space Administration and United States Geological Survey proposed an algorithm to retrieve LST from LANDSAT 8 data, the proposed algorithm was created in ERDAS IMAGINE

2014, and it can only be used to process LANDSAT 8 data because of the data complexity (Avdan and Jovanovska 2016).

Top of Atmospheric Spectral Radiance

The first step of the algorithm is the input of Band 10 from LANDSAT 8. In the background, the tool uses formulas taken from the USGS web page for retrieving the top of atmospheric (TOA) spectral radiance ($L\lambda$);

$$L\lambda = M_L * Q_{cal} + A_L - O_i \quad (1)$$

where M_L represents the band-specific multiplicative rescaling factor, Q_{cal} is the Band 10 image, A_L is the band-specific additive rescaling factor, and O_i is the correction for Band 10 (Barsi et al. 2014).

Conversion of Radiance to At-Sensor Temperature

After the digital numbers (DNs) are converted to reflection, the TIRS band data should be converted from spectral

radiance to brightness temperature (BT) using the thermal constants provided in the metadata file of the satellite images used in the algorithm as presented in Table 1. The following equation is used in the tool's algorithm to convert reflectance to BT (USGS 2013):

$$BT = \frac{K_2}{\ln \left[\left(K_1 / L\lambda \right) + 1 \right]} - 273.15 \quad (2)$$

where K_1 and K_2 stand for the band-specific thermal conversion constants from the metadata. For obtaining the results in Celsius, the radiant temperature is revised by adding the absolute zero (approx. -273.15 °C) (Xu and Chen 2004).

NDVI Method for Emissivity Correction

Calculating NDVI LANDSAT visible and near-infrared bands were used for calculating the Normal Difference Vegetation Index (NDVI). The importance of estimating the NDVI is essential since the amount of vegetation present is an important factor. The calculation of the NDVI is important because, afterward, the proportion of the vegetation (P_V) should be calculated, and they are highly related with the NDVI, and emissivity () should be calculated, which is related to the P_V :

$$NDVI = \frac{NIR \text{ (band 5)} - R \text{ (band 4)}}{NIR \text{ (band 5)} + R \text{ (band 4)}} \quad (3)$$

where NIR represents the near-infrared band (band 5) and R represents the red band (band 4).

Calculating the Proportion of Vegetation P_V is calculated according to Eq. (4). A method for calculating P_V suggests using the NDVI values for vegetation and soil ($NDVI_v = 0.5$ and $NDVI_s = 0.2$) to apply in global conditions (Wang et al. 2015; Sobrino et al. 2004).

$$P_V = \left(\frac{NDVI - NDVI_s}{NDVI_v - NDVI_s} \right)^2 \quad (4)$$

However, since the NDVI values differ for every area, the value for vegetated surfaces, 0.5, may be too low. Global values from NDVI can be calculated from at-surface reflectivities, but it would not be possible to establish global values in the case of an NDVI computed from TOA reflectivities, since $NDVI_v$ and $NDVI_s$ will depend on the atmospheric conditions (Jimenez et al. 2009).

Calculating Land Surface Emissivity The land surface emissivity (LSE (ϵ)) must be known in order to estimate LST, since the LSE is a proportionality factor that scales blackbody radiance (Planck's law) to predict emitted radiance, and it is the efficiency of transmitting thermal energy across the surface into the atmosphere (Jimenez et al. 2006). The determination of the ground emissivity is calculated conditionally (Sobrino et al. 2004).

$$\epsilon_\lambda = \epsilon_{v\lambda} P_V + \epsilon_{s\lambda} (1 - P_V) + C_\lambda \quad (5)$$

where ϵ_v and ϵ_s are the vegetation and soil emissivities, respectively, and C represents the surface roughness ($C = 0$ for homogenous and flat surfaces) taken as a constant value of 0.005 (Sobrino and Raissouni 2000).

The last step of retrieving the LST or the emissivity-corrected land surface temperature (T_s) is computed as follows:

$$T_s = \frac{BT}{\{1 + [(\lambda BT / \rho) \ln \epsilon_\lambda]\}} \quad (6)$$

where T_s is the LST in Celsius (°C), BT is at-sensor BT (°C), λ is the wavelength of emitted radiance (for which the peak response and the average of the limiting wavelength ($\lambda = 10.895$) (Markham and Barker 1985) will be used), ϵ_λ is the emissivity calculated in Eq. (5), and

$$P = h \frac{c}{\sigma} = 1.438 \times 10^{-2} m K \quad (7)$$

where σ is the Boltzmann constant (1.38×10^{-23} J/K), h is Planck's constant (6.626×10^{-34} J s), and c is the velocity of light (2.998×10^8 m/s) (Weng et al. 2004).

Ground-Based Air Pollutant Concentration Data

This section implies the collection of ground-based concentration data and their way of representation. There are several tools to collect the environmental pollution particulars (Chakraborty 2014); however, primary air pollutant (in $\mu\text{g}/\text{m}^3$) and daily average temperature (in °C) data were downloaded from a public domain of the West Bengal Pollution Control Board to measure the amount of pollution in places like RBU zone ($22^\circ 37' 54.025''$ N, $88^\circ 22' 44.299''$ E), VICT zone ($22^\circ 32'$

Table 1 Metadata of the satellite images of LANDSAT 8 (2018)

Type and band information	Constant	Value
Thermal constant, band 10	K_1	1321.08
	K_2	777.89
Rescaling factor, band 10	M_L	0.000342
	A_L	0.1
Correction, band 10	O_i	0.29

45.457" N, 88° 20' 29.246" E) of KMC, and Babupara zone (26° 44' 3.883" N, 88° 26' 28.471" E) of SMC quite precisely. These downloaded data were initially collected by the observation stations of West Bengal Pollution Control Board (n.d.) placed at different regions to represent air quality data with different characteristics where monitoring is performed based on automatic air quality control and information system. Available data were collected for three different periods throughout the year, post-monsoon (November and December 2018 and January 2019), pre-monsoon (March, April, and May 2019), and monsoon (July, August, and September 2019) to compare variant air pollutants in different seasons at two zones of Kolkata and one of Siliguri is a major criterion of this study. But it is necessary here to mention that data were not available for each pollutant mentioned in this work for each hour of all days throughout the three seasons; thereafter, for the sake of uniformity, we have tried to consider the data of 1st, 5th, 10th, 15th, 20th, 25th, and 30th day of each month. The data of each air pollutant were taken into consideration for two times (11 AM at day and 11 PM at night) as there is significant life changes that occur between day and night times like vehicle movement, the opening of industries, etc., contributing to day and night time variations for each zone.

Aerosol optical depth data are provided by Moderate Resolution Imaging Spectroradiometer (MODIS) that is generally used in research and development works and can reveal the distribution of particulate matter on a large regional scale to some extent (Gupta et al. 2006; Li et al. 2017). But, MODIS images cannot be obtained at every time (Levy et al. 2007), and also it is difficult to reveal variations of particulate matter concentrations for different time scales (seasonal, monthly, daily, or hourly). Besides, MODIS data are affected by clouds. Therefore, compared with the remotely sensed satellite images, near-ground observation data on air pollutant concentrations are more accurate and scientific and are used in this study.

Spatial-Temporal Characterizations of Air Pollutants

Total concentrations of five main pollutants (PM_{2.5}, PM₁₀, CO, NO₂, and SO₂) in the cities initially were estimated by averaging out available daily data into daily average, monthly averaged mean, and then into seasonal mean data for each of the pollutants. As this study gives emphasis on the seasonal variation of pollutants thus as a whole, for each season, an average of twenty-one datasets of each air pollutant was considered. The recorded amounts of all the pollutants were critically examined and shown with the help of a column diagram in the GIS platform. Later on, to study most variant pollutant concentration in the predefined

three seasons accordingly to regional meteorological characteristics, boxplots of the monthly PM_{2.5} and PM₁₀ concentrations have been created.

In different environmental forensic investigations, a variety of statistical analysis techniques can be involved. A relatively simple technique that can be used for explicit data analysis is the Spearman rank correlation coefficient (SRCC) (Thomas 2010). In early of the twentieth century, after giving the introduction of the rank correlation coefficient, Spearman delivered a considerable effort for obtaining its sampling distribution when the variables being correlated are independent. SRCC is a nonparametric technique for evaluating the degree of linear association or correlation between two random independent variables. There are many advantages of SRCC over other correlation coefficients. Firstly, as it is a nonparametric technique (Jerrold 2012); thus, it is unaffected by the distribution of the sample. Secondly, as the technique operates on the rank of the data rather than the available raw data, it is relatively insensitive to outliers and there is no requirement that data be collected over regular intervals. Thus, it can be used with very small sample sizes (Helena 2012) and also easy to apply. Hence, in this research work, Spearman's rank correlation method was applied between the average temperature of the day and the concentration of significant air pollutants like PM_{2.5} and CO by considering the rank values of the two concerned variables based on their corresponding available data for the same date and which is quite useful to gauge the environmental health and its projected impact on humans. Intuitively, Spearman's correlation between two variables will be high when observations have a similar rank between the two variables and low when observations have a dissimilar rank. Spearman's correlation coefficient is defined by Eq. (8):

$$r_s = 1 - \frac{6 \sum d_i^2}{n(n^2 - 1)} \quad (8)$$

where r_s is the Spearman rank correlation coefficient, d_i represents the difference between the ranks of corresponding variables at a particular date, and n denotes the number of observations. Moreover, SRCC is a technique which can be used to summarize the strength and direction (negative or positive) of a relationship between two random variables and to measure the degree of association between them. The Spearman rank correlation test does not carry any assumptions about the distribution of the data and is the appropriate correlation analysis when the variables are measured on a scale that is at least ordinal. The result will always be between +1 and -1; more specifically, values of r_s from 0 to +1 indicate a positive correlation between the two selected variables, whereas values of r_s from -1 to 0 indicate a negative correlation among observed variables (Thomas 2010; Gautheir 2010; Jerrold 2012).

Results and Discussion

Land Use/Land Cover Dynamics and Analysis of Land Surface Temperature

Over the study areas, it has been identified from decadal LULC classification that rapid land use changes basically initiated by the urbanization process (Figs. 2 and 3). For the KMC area, it is quite prominent that the built-up (built-up compact and built-up sparse) area that accounts for 85% of the area in the total LULC configuration in 2006 increased to 88% compact built-up area in 2016 (Table 2). Analysis using multi-dated satellite images reveals that the land cover categories and the rate of conversion from different classes to residential land use are extreme and it exhibits an unbalanced urban growth pattern.

As the SMC area is not an exception, the pattern of changes in LULC is also observed here. In a rapid appraisal of built-up, growth phenomenon within a city or large town is often significantly higher than the surrounding rural areas and it is also identified for the SMC. In this regard, it is quite necessary to mention that the percentage of area covered by compact built-up is 97% in 2016 as the sparse built-up area of 2006 has been converted into built-up compact area (Table 3).

Geo-spatially, it has been clearly understood that the emergence of new built-up areas fundamentally belongs to the vegetated area, water body, and agricultural land feeding pattern. In recent decades, these areas have undergone an accelerated process of urbanization, though the population densities and the extent of urbanization in different cities differ from

each other, but the rapid land use change initiated by the urbanization process increases traffic congestion as a result of a high vehicular movement contributing to air pollution. Most significantly urbanization transforms the natural land surfaces to modern LULC such as buildings, roads, and other impervious surfaces, making urban landscapes fragmented and complex which affects the inhabitability of cities (Alberti and Marzluff 2004). Besides, the incremental urbanization process brought about many eco-environmental problems, such as the drastic change of land use and development of urban heat islands (Jiang and Tian 2010).

The LST study reveals that in KMC and SMC areas, high temperature is associated mainly with built-up. In the KMC area, the high-temperature zones have been seen in the northern and central parts due to anthropogenic land use. Derived result from the LST analysis shows a temperature range from 29.033 to 19.001 °C in KMC. This illustrates the geographical and topographical LST allocation and represents the outline and strength of the distribution of built-up in and around the KMC. Considering in the SMC area the approximate surface temperature value ranges from 27.915 to 22.001 °C, it exposed the thermal variation in different LULC classes. The highest surface temperature was found in built-up areas and impervious surfaces such as industrial areas, as well as other man-made coatings (Fig. 4).

The urban heat pockets are mostly observed for both of the concerned areas that they are concentrated in built-up areas where residential and industrial land use practices are prevalent. Such a high temperature is an outcome of the increasing rate of built-up

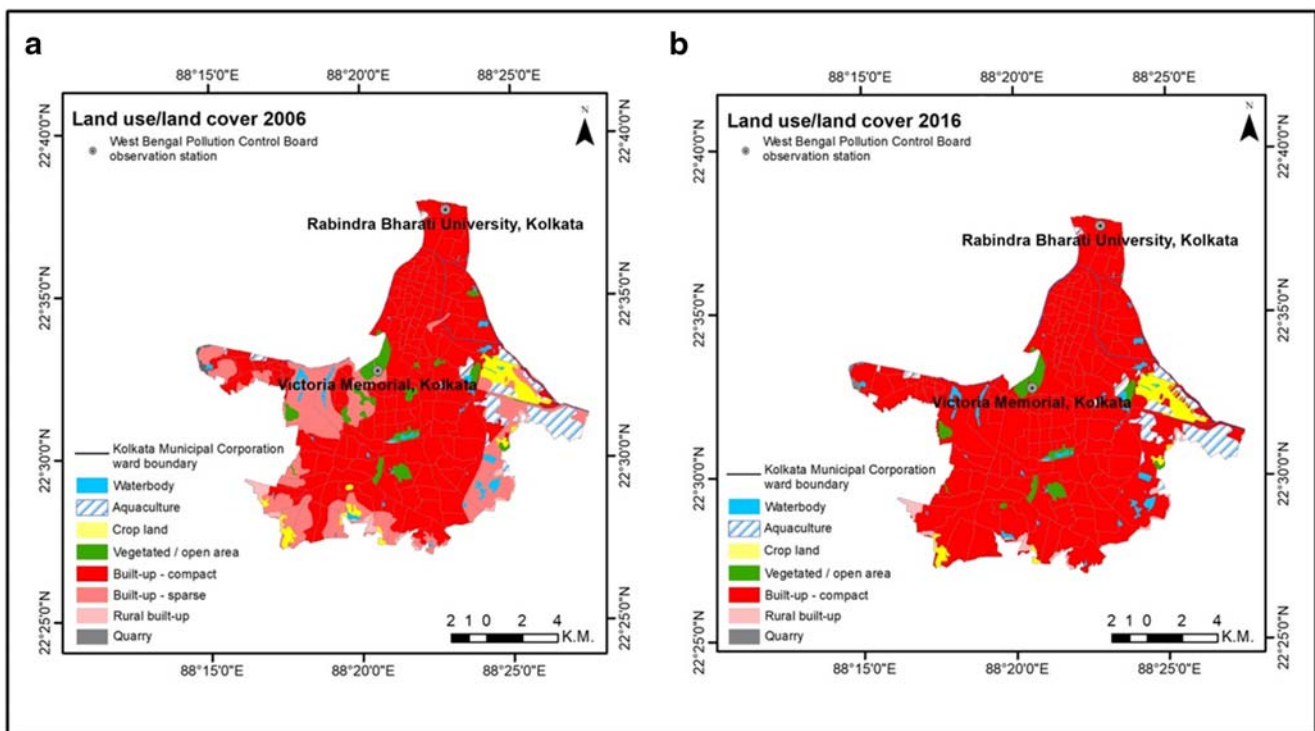


Fig. 2 Change in land use/land cover of Kolkata Municipal Corporation area, West Bengal, India, from 2006 (a) to 2016 (b)

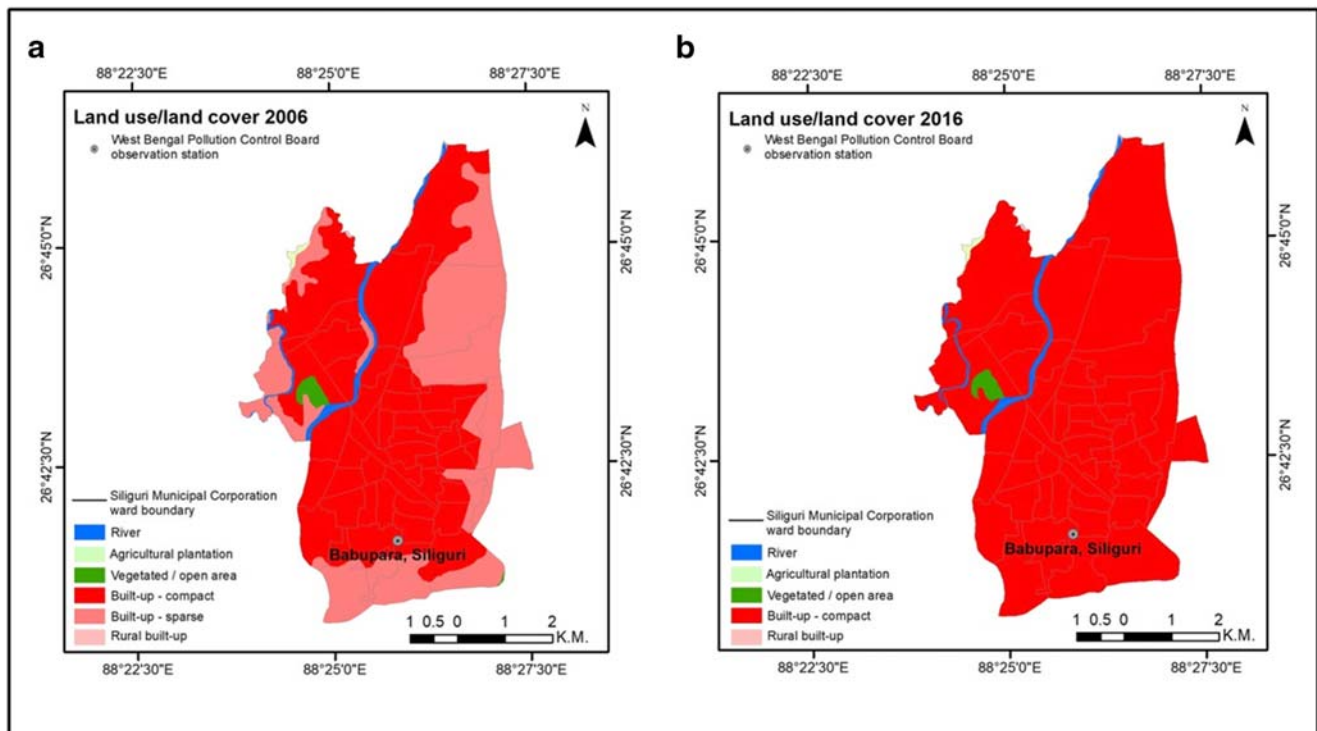


Fig. 3 Change in land use/land cover of Siliguri Municipal Corporation area, West Bengal, India, from 2006 (a) to 2016 (b)

development over the concerned areas (Kayet et al. 2016). This will enable us to assess the spatial changes in surface and gives an idea about near-surface temperature. Such higher temperatures are beneficial to pollutant diffusion (Huang et al. 2018).

Spatial-Temporal Distribution Changes of Air Pollutants

Seasonal Variations in Atmospheric Pollutants

Decadal LULC transformation and surface temperature results suggest systematic findings toward the presence of air

pollutants over the concerned regions. In this regard, observations were made over the recorded data to find out the differences of different air pollutants like $PM_{2.5}$, PM_{10} , NO_2 , SO_2 , and CO in places like RBU and VICT of Kolkata and Babupara of Siliguri at day (11 AM) and night (11 PM) separately for the post-monsoon season. It is seen from the column diagram (Fig. 5) that the presence of PM like $PM_{2.5}$ and PM_{10} in the RBU zone (363.5 and $295.4 \mu g/m^3$ respectively at daytime; 346.6 and $290.4 \mu g/m^3$ separately at night time) is significantly higher to the respective values in the Victoria Memorial zone (294.5 and $197.3 \mu g/m^3$ at day; 292.6 and $198.5 \mu g/m^3$ correspondingly at night) over the season. On

Table 2 Change in the area under different land use/land cover categories in Kolkata Municipal Corporation from 2006 to 2016

2006			2016		
Land use/land cover classes	Area in hectare	Area in percentage (%)	Land use/land cover classes	Area in hectare	Area in percentage (%)
Water body	452.413	2.425	Water body	188.946	1.013
Aquaculture	727.745	3.901	Aquaculture	727.733	3.901
Crop land	572.262	3.067	Crop land	489.205	2.622
Vegetated/open area	669.687	3.588	Vegetated/open area	506.723	2.716
Built-up compact	11,934.079	63.971	Built-up compact	16,460.855	88.237
Built-up sparse	4017.422	21.535	Built-up sparse	Built-up sparse class totally converted into built-up compact	
Rural built-up	250.019	1.340	Rural built-up	250.0183	1.340
Quarry	31.742	0.170	Quarry	31.889	0.171

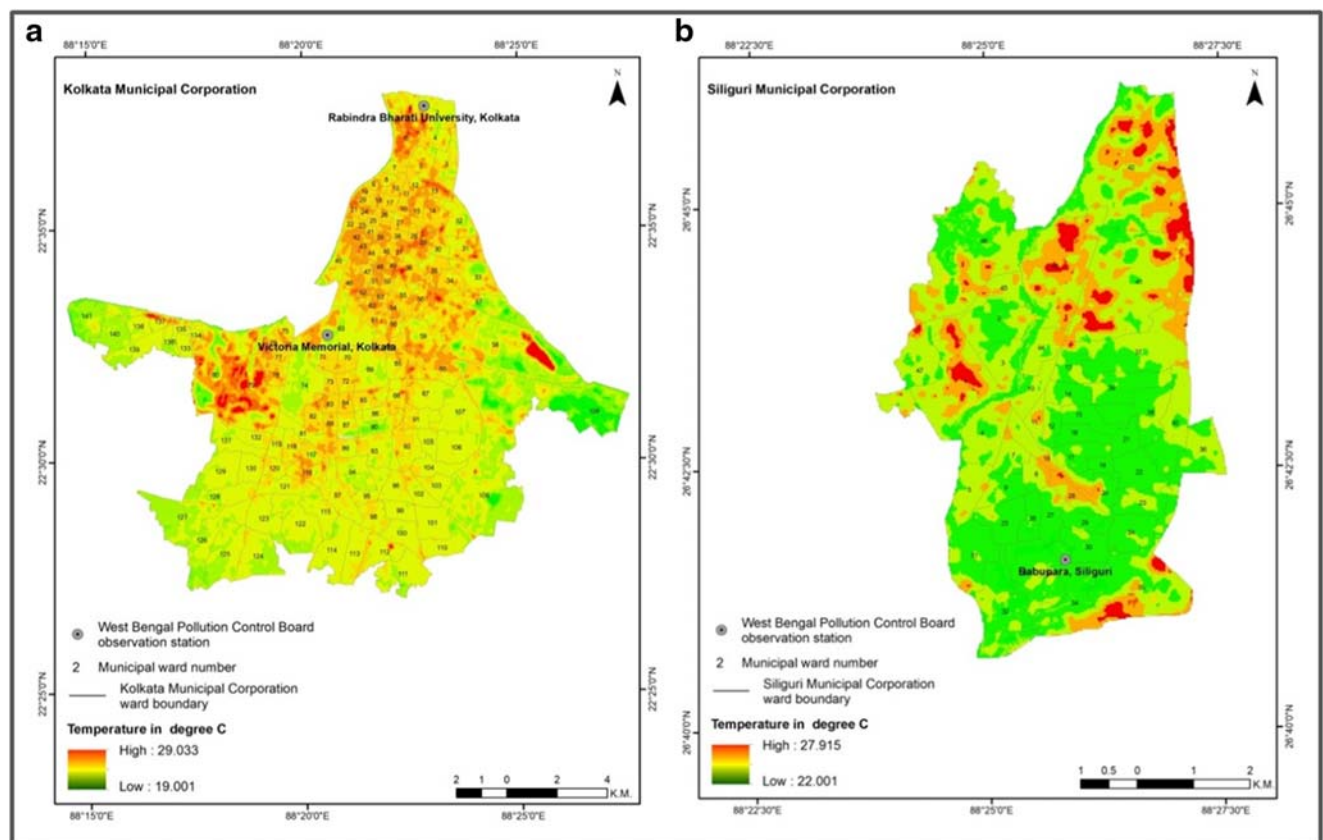
Table 3 Change in the area under different land use/land cover categories in Siliguri Municipal Corporation from 2006 to 2016

2006			2016		
Land use/land cover classes	Area in hectare	Area in percentage (%)	Land use/land cover classes	Area in hectare	Area in percentage (%)
River	70.916	1.914	River	70.916	1.914
Agricultural plantation	8.341	0.225	Agricultural plantation	8.341	0.225
Vegetated/open area	28.264	0.763	Vegetated/open area	27.200	0.734
Built-up compact	2296.840	61.977	Built-up compact	3598.401	97.097
Built-up sparse	1300.497	35.092	Built-up sparse	Built-up sparse class totally converted into built-up compact	
Rural built-up	1.109	0.030	Rural built-up	1.109	0.030

the contrary, the presence of selected pollutants is much less in the Babupara zone of Siliguri that is 183.7 and $168.8 \mu\text{g}/\text{m}^3$ at daytime and 187.9 and $172.9 \mu\text{g}/\text{m}^3$ at night time. Therefore, AQI of Siliguri is much better than the zones of Kolkata throughout the season both in day and night times. However, the presence of CO in the air of Victoria Memorial zone ($70.7 \mu\text{g}/\text{m}^3$) is almost three times greater than the other two zones (25.2 and $27.6 \mu\text{g}/\text{m}^3$ individually at RBU zone and Siliguri zone) mainly during the daytime and also it remains quite high ($83.7 \mu\text{g}/\text{m}^3$) in the air at night, which

makes the zone unhealthy over the post-monsoon period. The presence of SO_2 and NO_2 remained nearly constant for all the zones for both day and night times over the season.

To understand the variations of primary air pollutants in different zones of Kolkata and Siliguri at day (11 AM) and night (11 PM) separately, the available data were analyzed consciously for the pre-monsoon season. Figure 6 shows that the presence of PM like $\text{PM}_{2.5}$ and PM_{10} in the RBU zone (119.8 and $114.6 \mu\text{g}/\text{m}^3$ at daytime; 110.4 and $109.7 \mu\text{g}/\text{m}^3$ at night time) is much higher than the respective values in the

**Fig. 4** Land surface temperature distribution in Kolkata Municipal Corporation (a) and Siliguri Municipal Corporation (b)

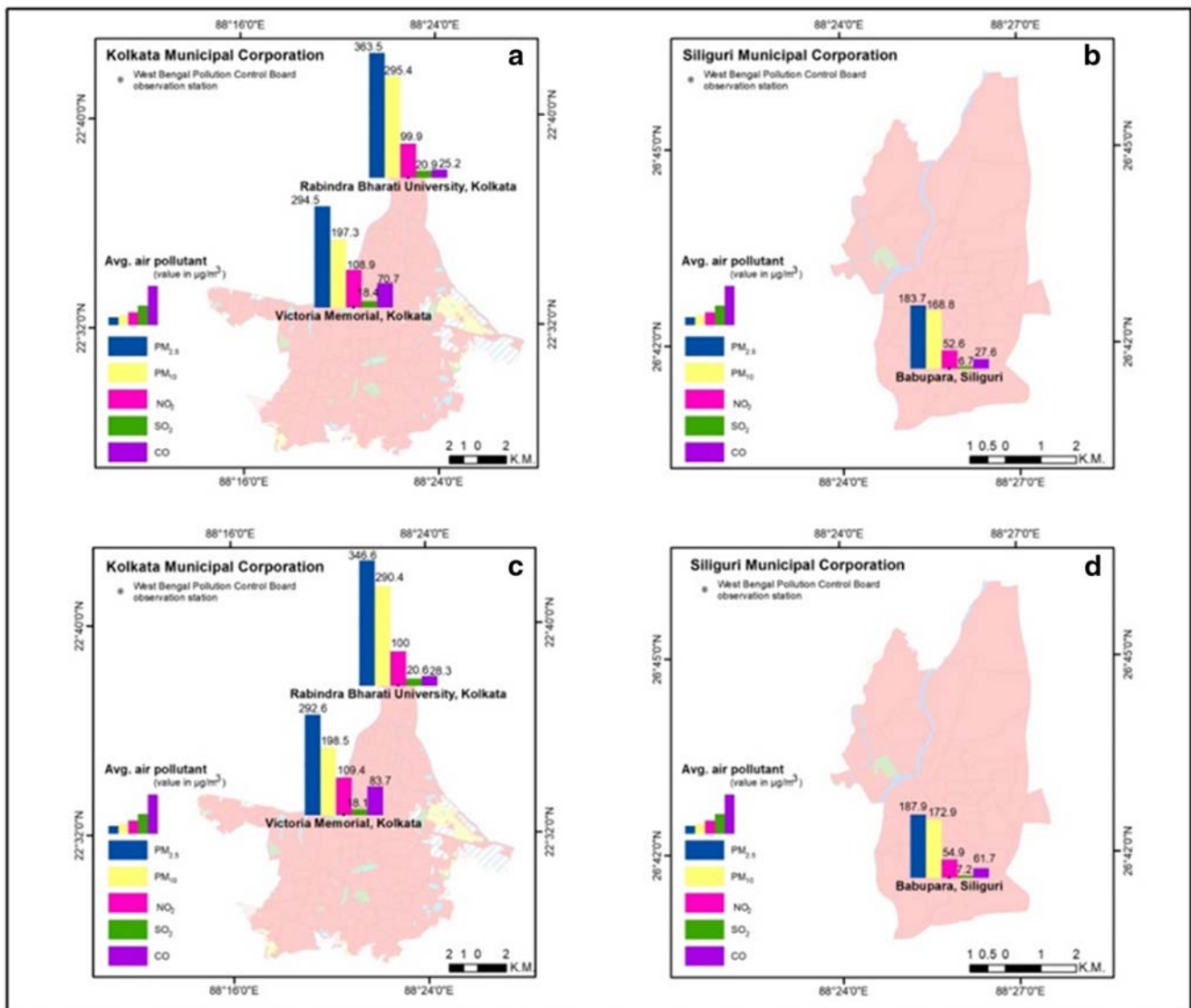


Fig. 5 Recorded average air pollutants of the selected observation stations at 11 AM in Kolkata Municipal Corporation (a) and Siliguri Municipal Corporation (b) and at 11 PM in Kolkata Municipal Corporation (c) and Siliguri Municipal Corporation (d) for the post-monsoon season

Babupara zone ($87.7 \mu\text{g}/\text{m}^3$ for both of the PM at day; 93.5 and $89.3 \mu\text{g}/\text{m}^3$ respectively at night) and is about more or less double the pollutant values in the Victoria Memorial zone (71.2 and $65.3 \mu\text{g}/\text{m}^3$ singly during the day; 65.1 and $63.1 \mu\text{g}/\text{m}^3$ correspondingly at night) over the season. The presence of CO in the air of Victoria Memorial zone and Babupara zone is nearly equal to $40 \mu\text{g}/\text{m}^3$ during day and night which is relatively higher than the amount present in the RBU during the day ($16.2 \mu\text{g}/\text{m}^3$) and night ($21.2 \mu\text{g}/\text{m}^3$) for the period. The presence of SO_2 is almost constant ($< 10 \mu\text{g}/\text{m}^3$) for all the zones for both day and night times, and the presence of NO_2 in the air is fairly higher for the RBU zone ($> 50 \mu\text{g}/\text{m}^3$) as compared to the Victoria Memorial zone ($38.9 \mu\text{g}/\text{m}^3$ at daytime and $33.8 \mu\text{g}/\text{m}^3$ at night time

separately) and Babupara zone ($38.7 \mu\text{g}/\text{m}^3$ and $40.2 \mu\text{g}/\text{m}^3$) for both day and night times in the season.

The deviations of different air pollutants in RBU and VICT of Kolkata and Babupara of Siliguri at day (11 AM) and night (11 PM) are distinctly shown in (Fig. 7) for the monsoon season. It exhibits that the presence of PM like $\text{PM}_{2.5}$ and PM_{10} in the RBU zone (56.5 and $66.9 \mu\text{g}/\text{m}^3$ singly at day; 60.9 and $70.4 \mu\text{g}/\text{m}^3$ respectively at night) is slightly higher to the respective values in Victoria Memorial (40.5 and $47.5 \mu\text{g}/\text{m}^3$ of daytime; 40.6 and $46.3 \mu\text{g}/\text{m}^3$ of night time) and Babupara zones (30.3 and $35.8 \mu\text{g}/\text{m}^3$ during the day; 32.6 and $37.1 \mu\text{g}/\text{m}^3$ during the night) over the season. However, in this period, the recorded presence of PM is quite satisfactory, according to international standards in all zones under consideration. The presence of CO in the air of Victoria Memorial

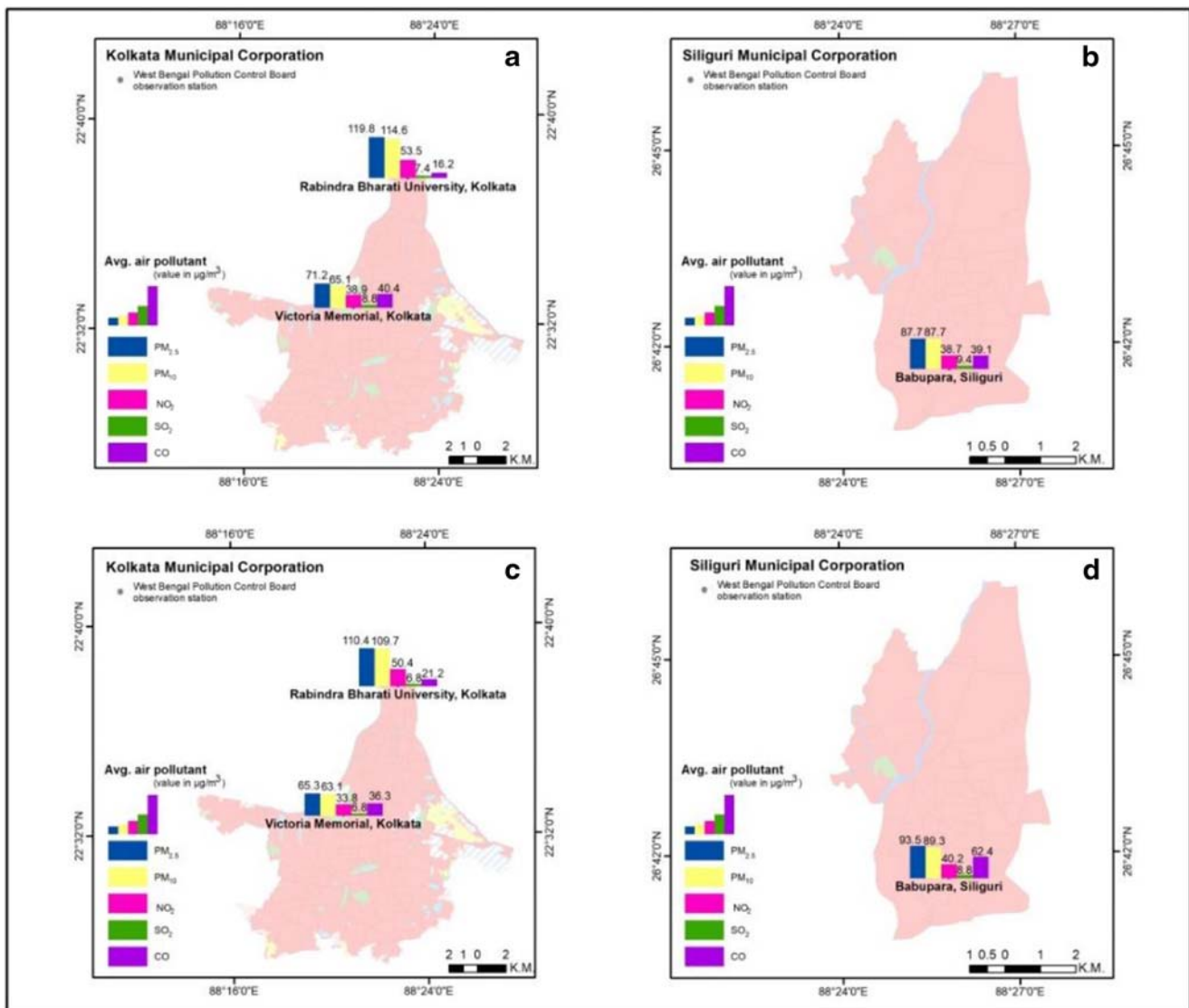


Fig. 6 Recorded average air pollutants of the selected observation stations at 11 AM in Kolkata Municipal Corporation (a) and Siliguri Municipal Corporation (b) and at 11 PM in Kolkata Municipal Corporation (c) and Siliguri Municipal Corporation (d) for the pre-monsoon season

zone ($52.4 \mu\text{g}/\text{m}^3$ at daytime; $60.3 \mu\text{g}/\text{m}^3$ at night time) is significantly higher than in RBU ($11.4 \mu\text{g}/\text{m}^3$ at day; $16.9 \mu\text{g}/\text{m}^3$ at night respectively) and Babupara zones both in the daytime ($20.4 \mu\text{g}/\text{m}^3$) and night time ($39 \mu\text{g}/\text{m}^3$) over the whole monsoon season. The presence of SO_2 ($< 10 \mu\text{g}/\text{m}^3$ in RBU zone and nearly $5 \mu\text{g}/\text{m}^3$ in two other zones) and NO_2 ($< 40 \mu\text{g}/\text{m}^3$) remained constant for all zones for both day and night times for the entire season.

Considerable seasonal changes in contaminant content for each study period show changes in concentrations of $\text{PM}_{2.5}$, PM_{10} , SO_2 , NO_2 , and CO in urban areas. In the post-monsoon season, the soil is dry and there is less vegetation cover, so it is easier for ground dust to enter the air; additionally, vehicular emissions and coal combustion in industries produce a great deal of polluting the air. The higher concentrations of particles

of both sizes were found in the post-monsoon (winter) period and the lowest ones in the monsoon season and their concentrations demonstrated similar values practically in the two concerned cities. Cumulative action of industrial sources and unfavorable weather conditions affects the low dilution and scattering of air pollution in winter (Guan et al. 2019). But, the natural factor dominates both the post-monsoon and pre-monsoon seasons, especially north-eastern wind that contributes to the formation of strong whirls during the post-monsoon, resulting in the capture of sand and silt and their emission into the air, leading to high levels of PM_{10} and $\text{PM}_{2.5}$. Besides, less precipitation, lower air temperature, and low height of the planetary boundary layer as well as the feeble winds in winter may increase pollution (Xu et al. 2016). Also, secondary nitrates and sulfates tend to accumulate in winter

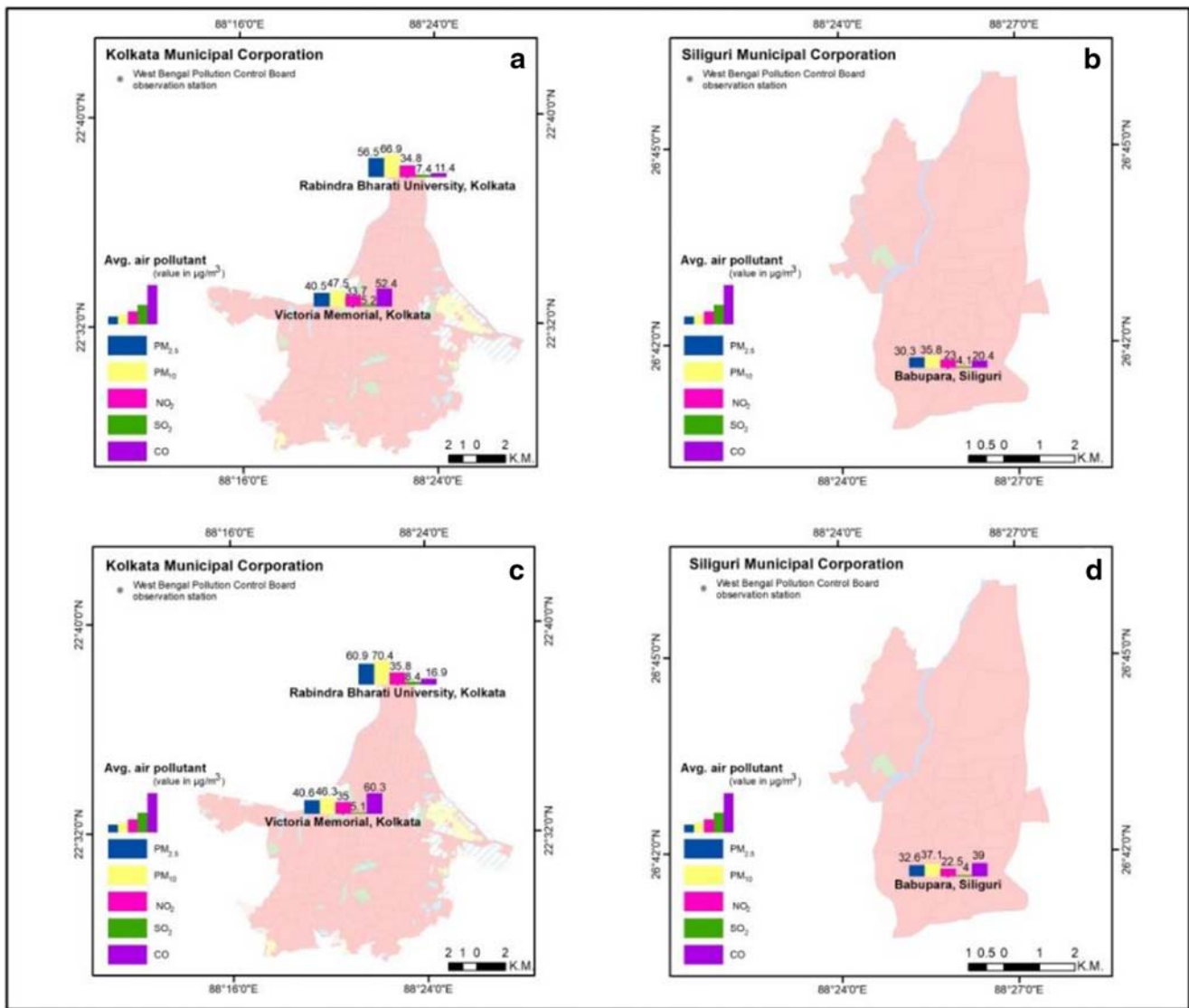


Fig. 7 Recorded average air pollutants of the selected observation stations at 11 AM in Kolkata Municipal Corporation (a) and Siliguri Municipal Corporation (b) and at 11 PM in Kolkata Municipal Corporation (c) and Siliguri Municipal Corporation (d) for the monsoon season

due to the lower height of the planetary boundary layer and small amount of precipitation (Tambo et al. 2016). In winter, PM_{2.5} concentration reached peak practically in the cities (with maximum values in RBU zone (363.5 µg/m³ at daytime; 346.6 µg/m³ at night time)). NO₂ and CO concentrations demonstrated similar seasonal fluctuations, while the highest concentrations were in the post-monsoon phase and the lowest ones in the monsoon. CO readings, particularly in the VICT zone, are observed to be very high in the post-monsoon season (83.7 µg/m³), which might be caused by increases in transportation. These seasonal fluctuations of pollutants reflect the impact of meteorological conditions and emissions. Meteorological conditions characterized by slower wind speeds and shallow mixed layers, that more often occur in winter, retain pollutants near the surface and lead to the high

concentrations (Christensen and Pringle 2012). Similarly, SO₂ concentrations were characterized by strong seasonal variation with maximum values in winter in the RBU zone (20.9 µg/m³) during the daytime. The primary source of SO₂ is burning of all sulfur containing fuel types like oil and diesel fuel (Chen et al. 2016).

Monthly Spatial Differentiation of PM_{2.5} and PM₁₀

To examine the monthly characteristics of the most variant seasonal pollutants, boxplots of PM_{2.5} and PM₁₀ concentrations were created. Figure 8 shows the boxplots of the monthly PM_{2.5} and PM₁₀ concentrations in three different zones. The interquartile ranges, the distance between the third and first quartiles, of PM_{2.5} and PM₁₀ in post-monsoon months,

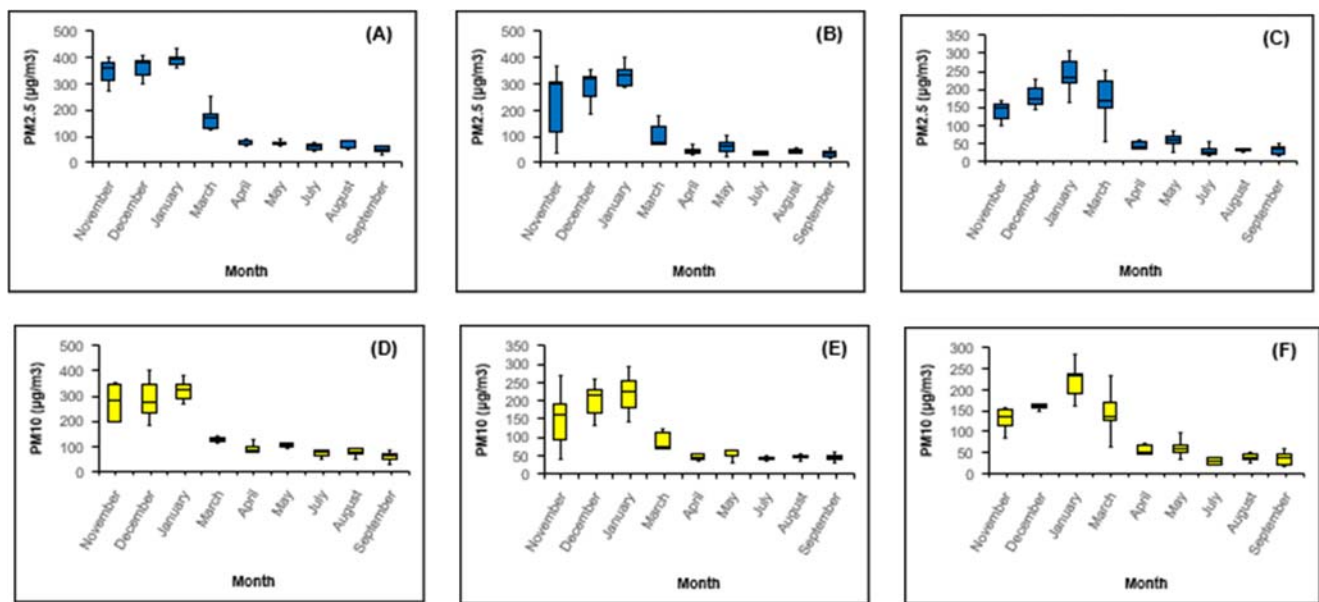


Fig. 8 Boxplots of average monthly concentrations of $PM_{2.5}$ in RBU (a), VICT (b), and SILG (c) zones and average monthly concentrations of PM_{10} in RBU (d), VICT (e), and SILG (f) zones for the pre-monsoon

(November and December 2018 and January 2019), pre-monsoon (March, April, and May 2019), and monsoon (July, August, and September 2019) seasons

are one- or two-fold higher than those in pre-monsoon (summer) and monsoon months, respectively, for the places. Both of the $PM_{2.5}$ and PM_{10} boxplots show a similar trend.

Due to major weather changes, diffusion conditions that affect climate are better in summer and autumn (Neumann-Hauf and Halbritter 1982). Thus, $PM_{2.5}$ concentrations are relatively low. Seasonal variation of PM_{10} is also similar. The relation between $PM_{2.5}$ and PM_{10} is often used to characterize the primary atmospheric processes in the local environment (Filonchik et al. 2016). $PM_{2.5}$ and PM_{10} are closely related since $PM_{2.5}$ contributes considerably to the total PM_{10} content in the atmosphere (Naser et al. 2008; Zhao et al. 2019). The size of atmospheric particulate matter is important as a determinant factor for how long the particles remain in the atmosphere and where they subsequently reside in human respiratory passages. As compared with PM_{10} , $PM_{2.5}$ may cause more severe consequences for human health due to its small size, allowing it to penetrate deep into the lungs

(Filonchik and Hurynovich 2020). The higher values of $PM_{2.5}$ and PM_{10} are usually inherent to anthropogenic activity and formation of secondary particles due to burning of hydrocarbon fuel and may also be attributed to vehicle emissions and secondary particles, formed through photochemical processes at high temperatures (Kishore et al. 2019). Upon analysis of $PM_{2.5}$ and PM_{10} values, it may be established that the main pollutant of selected regions is coarser particles as measured by PM_{10} .

Spearman's Rank Correlation to Address Environmental Pollution

For a better understanding, the Spearman rank correlation coefficient method is used in this work to describe the relationship (whether linear or not) between two variables, i.e., temperature and pollutants ($PM_{2.5}$ and CO), using a monotonic function. As this work deals with two ranked random

Table 4 Spearman's rank correlation values for temperature vs. significant air pollutants in different seasons

	Seasons								
	Post-monsoon season (November and December 2018 and January 2019)			Pre-monsoon season (March, April, and May 2019)			Monsoon season (July, August, and September 2019)		
	Zones			Zones			Zones		
	RBU	VICT	SILG	RBU	VICT	SILG	RBU	VICT	SILG
r_s values for temperature vs. $PM_{2.5}$	0.07	0.03	0.03	0.03	0.13	0.34	0.63	0.33	0.63
r_s values for temperature vs. CO	0.76	-0.03	-0.03	-0.03	0.32	0.50	0.49	0.46	0.27

variables, Spearman's correlation is used as it considers the rank values of the two concerned variables based on their corresponding available data for the same date. Table 4 shows satisfactory values of SRCC indicating that there is a good correlation between average temperature and $PM_{2.5}$ particularly in the monsoon season for all three zones (0.63 for RBU and SILG zones, 0.33 of VICT zone). A positive correlation is also observed for $PM_{2.5}$ with temperature in the pre-monsoon season in the SILG zone (0.34). However, such a relationship is not observed for the other two zones in Kolkata. A good relationship is furthermore observed between average temperature and CO in all the three study zones over the three seasons (0.76 for the RBU zone in post-monsoon season, 0.32 for the VICT zone and 0.50 for the SILG zone in the pre-monsoon season, nearly 0.50 for the RBU and VICT zone in the monsoon season). Positive correlations may indicate the contemporary status of the air quality as well as the environmental state in and around the studied area. Presently, such pollutants coming out from different sources are also raising temperatures. Therefore, the increasing level of these PM values and other pollutants is alarming.

Conclusion

Analyses have shown that the presence of PM, particularly $PM_{2.5}$ and PM_{10} , becomes very high in the post-monsoon season in Kolkata (> 300 on average). In the pre-monsoon and monsoon seasons, PM concentrations are observed to be moderate (nearly 100) and satisfactory (around 50), respectively. These $PM_{2.5}$ and PM_{10} cause health hazards like breathing problems, respiratory system disorder, allergy, asthma, sinus, headache, and bronchitis, to name a few. It affects not only children and elderly persons but also the younger generations. It is also observed that due to intense urbanization, the land and near-surface temperature of the studied areas is also increasing. This increase of temperature directly affects the presence of CO in the air—as a positive correlation is obtained between these two through SRCC in three zones over the seasons. Increased levels of CO can reduce the amount of oxygen carried by hemoglobin in red blood cells in the body. The result is that vital organs, such as the brain, nervous tissues, and the heart, do not receive enough oxygen to work properly. Not more than 2.5% of hemoglobin can be bound to CO before some health effects become noticeable. At very high concentrations of CO, up to 40% of the hemoglobin can be bound to it. This level will almost certainly kill humans (Department of Environment Government of West Bengal, West Bengal Pollution Control Board Kolkata 2002).

Raised levels of pollutants can have significant impacts on human health. The municipal corporations should come forward to manage this unavoidable situation by taking necessary steps like implementing national fuel quality standards and

promoting alternative fuels, supporting the implementation of tighter vehicle emission standards, encouraging citizens to plant trees under afforestation programs, and modifying our habits and lifestyles toward being environment friendly. Thus, KMC and SMC should adopt and implement major initiatives in the near future.

Atal Mission for Rejuvenation and Urban Transformation (AMRUT)

The purpose of AMRUT is to (a) increase the amenity value of cities by developing greenery and well-maintained open spaces (e.g., parks) and (b) reduce pollution by switching to public transport or constructing facilities for non-motorized transport (e.g., walking and cycling).

Green City Mission

A green city derives its energy from renewable sources like solar and wind and distributes that energy through efficient and reliable micro-grids. Focused on three key elements: buildings, energy, and transportation, the campaign aims to help cities accelerate their transition to a cleaner, healthier, and more economically viable future through improvements in efficiency, investments in renewable technology, and regulation reform.

Capacities

The Swiss Agency for Development and Cooperation (SDC) through its global program climate change in India has decided to support city authorities in addressing upcoming challenges due to climate change through the Capacities project. The goal of the Capacities project is lower greenhouse gas emission growth path achieved and resilience to climate increase in select Indian cities. SMC has been selected as part of the project by SDC along with Coimbatore, Rajkot, and Udaipur. In the coming years, KMC must take part in this program.

Acknowledgments We are grateful to the West Bengal Pollution Control Board, Government of West Bengal, for continuously uploading daily temperature (in °C) and air pollutant (in $\mu\text{g}/\text{m}^3$) data in their official website. We would like to appreciate the Kolkata and Siliguri Municipal Corporations for sharing information about their ongoing projects and schemes. The authors are also thankful to the Editor-in-Chief, *Journal of Geovisualization and Spatial Analysis*, for his valuable suggestions and recommendation.

Compliance with Ethical Standards

This research work is carried out in compliance with transparency, moral values, honesty, and hard work. No human participation or animals are involved in this research work.

Conflict of Interest The authors declare that they have no competing interests.

Ethical Approval As per the literature review, this is neither a repetition of any work nor copied key data from other's work. The methodology, findings, and conclusions made here belong to original research work as per our knowledge and belief.

Informed Consent Every step of processing for publication informed to all co-authors of this paper at the earliest, and everything is carried out with collective decision and consent.

References

- Alberti M, Marzluff J (2004) Ecological resilience in urban ecosystems: linking urban patterns to ecological and human function. *Urban Ecosyst* 7(3):241–265. <https://doi.org/10.1023/B:UECO.0000044038.90173.c6>
- Avdan Q, Jovanovska G (2016) Algorithm for automated mapping of land surface temperature using LANDSAT 8 satellite data. *Journal of Sensors* 2016:1–8. <https://doi.org/10.1155/2016/1480307>
- Barsi JA, Schott JR, Hook SJ, Raqueno N, Markham B, Radocinski R (2014) Landsat-8 thermal infrared sensor (TIRS) vicarious radiometric calibration. *Remote Sens* 6(11):1607–11626. <https://doi.org/10.3390/rs6111607>
- Chakraborty A (2014) Effect of air pollution on public health: the case of vital traffic junctions under Kolkata Municipal Corporation. *Journal of Studies in Dynamics and Change* 1(3):125–133
- Chen W, Tang H, Zhao H (2016) Urban air quality evaluations under two versions of the national ambient air quality standards of China. *Atmospheric Pollution Research* 7(1):49–57. <https://doi.org/10.1080/1943815X.2016.1150301>
- Christensen MK, Pringle JM (2012) The frequency and cause of shallow winter mixed layers in the Gulf of Maine. *Journal of Geophysical Research*:117 <https://doi.org/10.1029/2011JC007358>
- D'amato G, Pawankar R, Vitale C et al (2016) Climate change and air pollution: effects on respiratory allergy. *Allergy Asthma and Immunology Research* 8(5):391–395. <https://doi.org/10.4168/aa.2016.8.5.391>
- De SM, Katsouyanni K, Michelozzi P (2013) Climate change, extreme weather events, air pollution and respiratory health in Europe. *Eur Respir J* 42(3):826–843. <https://doi.org/10.1183/09031936.00074712>
- Department of Environment Government of West Bengal, West Bengal Pollution Control Board Kolkata (2002) Health effects of air pollution: a study of Kolkata report
- Filonchik M, Hurynovich V (2020) Spatial distribution and temporal variation of atmospheric pollution in the South Gobi Desert, China, during 2016–2019. *Environ Sci Pollut Res* 27:26579–26593. <https://doi.org/10.1007/s11356-020-09000>
- Filonchik M, Yan H (2018) The characteristics of air pollutants during different seasons in the urban area of Lanzhou, Northwest China. *Environ Earth Sci* 77(22):763. <https://doi.org/10.1007/s12665-018-7925-1>
- Filonchik M, Yan H, Yang S, Hurynovich V (2016) A study of PM_{2.5} and PM₁₀ concentrations in the atmosphere of large cities in Gansu Province, China, in summer period. *Journal of Earth System Science* 125(6):1175–1187. <https://doi.org/10.1007/s12040-016-0722-x>
- Gauthier DT (2010) Detecting trends using Spearman's rank correlation coefficient. *Environ Forensic* 4(2):359–362. <https://doi.org/10.1006/enfo.2001.0061>
- Guan Q, Yang Y, Luo H, Zhao R, Pan N, Lin J, Yang L (2019) Transport pathways of PM₁₀ during the spring in northwest China and its characteristics of potential dust sources. *J Clean Prod* 237:117746. <https://doi.org/10.1016/j.jclepro.2019.117746>
- Gupta P, Christopher SA, Wang J, Gehrig R, Lee Y, Kumar N (2006) Satellite remote sensing of particulate matter and air quality assessment over global cities. *Atmos Environ* 40:5880–5892. <https://doi.org/10.1016/j.atmosenv.2006.03.016>
- Gupta RC (2006) Environmental and infrastructural sustainability: major challenges facing Indian metropolitan cities. Sustainable Urban Development. Concept Publishing Company, New Delhi, India, pp 3–11
- Huang Y, Yan Q, Zhang C (2018) Spatial-temporal distribution characteristics of PM_{2.5} in China in 2016. *Journal of Geovisualization and Spatial Analysis* 2:12. <https://doi.org/10.1007/s41651-018-0019-5>
- Jerrold H (2012) Significance testing of the Spearman rank correlation coefficient. *J Am Stat Assoc* 339(67):578–580. <https://doi.org/10.1080/01621459.1972.10481251>
- Jiang J, Tian G (2010) Analysis of the impact of land use/land cover change on land surface temperature with remote sensing. *Procedia Environ Sci* 2:571–575. <https://doi.org/10.1016/j.proenv.2010.10.062>
- Jimenez JC, Sobrino JA, Plaza A et al (2009) Comparison between fractional vegetation cover retrievals from vegetation indices and spectral mixture analysis: case study of PROBA/CHRIS data over an agricultural area. *Sensors* 9:768–793. <https://doi.org/10.3390/s90200768>
- Jimenez JC, Sobrino JA, Gillespie A et al (2006) Improved land surface emissivities over agricultural areas using ASTER NDVI. *Remote Sens Environ* 103:474–487. <https://doi.org/10.1016/j.rse.2006.04.012>
- Kayet N, Pathak K, Chakrabarty A, Sahoo S (2016) Urban heat island explored by co-relationship between land surface temperature vs multiple vegetation indices. *Spat Inf Res* 24:515–529. <https://doi.org/10.1007/s41324-016-0049-3>
- Kazimuddin A, Banerjee L (2000) Fighting for air. *Down to Earth* (July 31)
- Kishore N, Srivastava AK, Nandan H, Pandey CP, Agrawal S, Singh N, Soni VK, Bisht DS, Tiwari S, Srivastava MK (2019) Long-term (2005–2012) measurements of near-surface air pollutants at an urban location in the Indo Gangetic Basin. *Journal of Earth System Science* 28(3):55. <https://doi.org/10.1007/s12040-019-1070-4>
- Levy RC, Remer LA, Mattoo S, Vermote EF, Kaufman YJ (2007) Second-generation operational algorithm: retrieval of aerosol properties over land from inversion of moderate resolution imaging spectroradiometer spectral reflectance. *Journal of Geophysical Research: Atmospheres* 112:319–321. <https://doi.org/10.1029/2006jd007811>
- Li X K, Zhang CR, Li WD et al (2017) Evaluating the use of DMSP/OLS nighttime light imagery in predicting PM_{2.5} concentrations in the northeastern United States. *Remote Sensing* 9:620. <https://doi.org/10.3390/rs9060620>
- Markham BL, Barker JL (1985) Spectral characterization of the Landsat Thematic Mapper sensors. *Int J Remote Sens* 6(5):697–716. <https://doi.org/10.1080/01431168508948492>
- Mondal R, Sen GK, Chatterjee M, Sen BK, Sen S (2000) Ground level concentration of nitrogen oxides (NO_x) at some traffic intersection points in Calcutta. *Atmos Environ* 34:629–633. [https://doi.org/10.1016/S1352-2310\(99\)00216-2](https://doi.org/10.1016/S1352-2310(99)00216-2)
- Mukherjee A, Mukherjee G (1998) Occupational exposure of the traffic personnel of Calcutta to lead and carbon monoxide. *Pollut Res* 17(4):359–362
- Naser T, Yoshimura Y, Sekiguchi K, Wang Q, Sakamoto K (2008) Chemical composition of PM_{2.5} and PM₁₀ and associated polycyclic aromatic hydrocarbons at a roadside and an urban background area in Saitama, Japan. *Asian Journal of Atmospheric Environment* 2(2): 90–101. <https://doi.org/10.5572/ajae.2008.2.2.090>

- National Remote Sensing Centre Bhuvan-earth observation data (n.d.). Retrieved from <https://bhuvan-app3.nrsc.gov.in/data/download/index.php>
- Neumann-Hauf G, Halbritter G (1982) Site and season-specific variations of the atmospheric pollutant transport and deposition on the local and regional scale. *Sci Total Environ* 23:91–96. [https://doi.org/10.1016/0048-9697\(82\)90124-3](https://doi.org/10.1016/0048-9697(82)90124-3)
- Ren C, Park SK, Vokonas PS, Sparrow D, Wilker E, Baccarelli A, Suh HH, Tucker KL, Wright RO, Schwartz J (2010) Air pollution and homocysteine: more evidence that oxidative stress-related genes modify effects of particulate air pollution. *Epidemiology* 21:198–206. <https://doi.org/10.1097/EDE.0b013e3181cc8bfc>
- Siddhartha K, Mukherjee S (2004) Cities, urbanization and urban systems. Kishalaya Publications, Delhi, pp 179–239
- Sobrino JA, Jimenez-Munoz JC, Paolini L (2004) Land surface temperature retrieval from LANDSAT TM5. *Remote Sens Environ* 90(4): 434–440. <https://doi.org/10.1016/j.rse.2004.02.003>
- Sobrino JA, Raissouni N (2000) Toward remote sensing methods for land cover dynamic monitoring: application to Morocco. *Int J Remote Sens* 21(2):353–366. <https://doi.org/10.1080/014311600210876>
- Spiroska J, Rahman MA, Pal S (2011) Air pollution in Kolkata: an analysis of current status and interrelation between different factors. *SEEU Review* 8(1):182–214. <https://doi.org/10.2478/v10306-012-0012-7>
- Tambo E, Duo-Quan W, Zhou XN (2016) Tackling air pollution and extreme climate changes in China: implementing the Paris climate change agreement. *Environ Int* 95:152–156. <https://doi.org/10.1016/j.envint.2016.04.010>
- UNEP (1999) Global environment outlook. Earthscan, London
- USGS (2013) http://landsat.usgs.gov/Landsat8_Using_Product.php
- USGS earth explorer-satellite images (n.d.). Retrieved from <https://earthexplorer.usgs.gov>
- Wang F, Qin Z, Song C, Tu L, Karnieli A, Zhao S (2015) An improved mono-window algorithm for land surface temperature retrieval from Landsat 8 thermal infrared sensor data. *Remote Sens* 7(4):4268–4289. <https://doi.org/10.3390/rs70404268>
- Weng Q, Lu D, Schubring J (2004) Estimation of land surface temperature-vegetation abundance relationship for urban heat island studies. *Remote Sens Environ* 89(4):467–483. <https://doi.org/10.1016/j.rse.2003.11.005>
- West Bengal Pollution Control Board-air pollutant data (n.d.). Retrieved from https://app.cpcbcr.com/AQI_India/
- WHO (2002) World health report. World health organization, Geneva, Switzerland
- Xie Y, Dai H, Dong H, Hanaoka T, Masui T (2016) Economic impacts from PM_{2.5} pollution-related health effects in China: a provincial level analysis. *Environmental Science & Technology* 50(9):4836–4843. <https://doi.org/10.1021/acs.est.5b05576>
- Xu HQ, Chen BQ (2004) Remote sensing of the urban heat island and its changes in Xiamen City of SE China. *J Environ Sci* 16:276–281
- Xu W, Wu Q, Liu X, Tang A, Dore AJ, Heal MR (2016) Characteristics of ammonia, acid gases, and PM_{2.5} for three typical land-use types in the North China plain. *Environ Sci Pollut Res* 23(2):1158–1172. <https://doi.org/10.1007/s11356-015-5648-3>
- Zhao D, Chen H, Yu E et al (2019) PM_{2.5}/PM₁₀ ratios in right economic regions and their relationship with meteorology in China. *Advances in Meteorology*. <https://doi.org/10.1155/2019/5295726>

Publisher's Note Springer Nature remains neutral with regard to jurisdictional claims in published maps and institutional affiliations.